ADVANCED FUNCTIONAL MATERIALS

Supporting Information

for *Adv. Funct. Mater.,* DOI: 10.1002/adfm.201803567

Platelet-Inspired Nanocells for Targeted Heart Repair After Ischemia/Reperfusion Injury

*Teng Su, Ke Huang, Hong Ma, Hongxia Liang, Phuong-Uyen Dinh, Justin Chen, Deliang Shen, Tyler A. Allen, Li Qiao, Zhenhua Li, Shiqi Hu, Jhon Cores, Brianna N. Frame, Ashlyn T. Young, Qi Yin, Jiandong Liu, Li Qian, Thomas G. Caranasos, Yevgeny Brudno, Frances S. Ligler, and Ke Cheng**

Supporting Information

Platelet-Inspired Nano-Cells for Targeted Heart Repair After Ischemia/Reperfusion Injury

*Teng Su, Ke Huang, Hong Ma, Hongxia Liang, Phuong-Uyen Dinh, Justin Chen, Deliang Shen, Tyler A. Allen, Li Qiao, Zhenhua Li, Shiqi Hu, Jhon Cores, Brianna N. Frame, Ashlyn T. Young, Qi Yin, Jiandong Liu, Li Qian, Thomas G. Caranasos, Yevgeny Brudno, Frances S. Ligler, Ke Cheng**

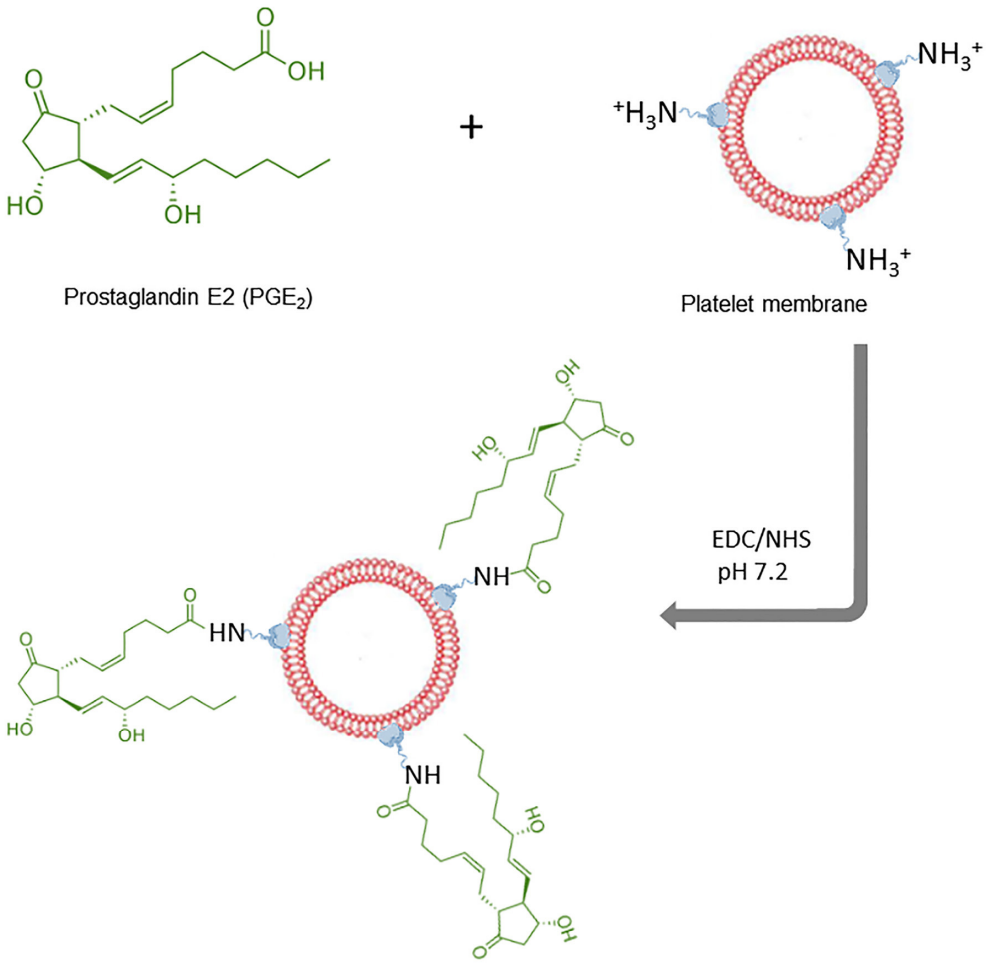

Figure S1. Synthesis of the PGE_2-platelet membrane conjugates.

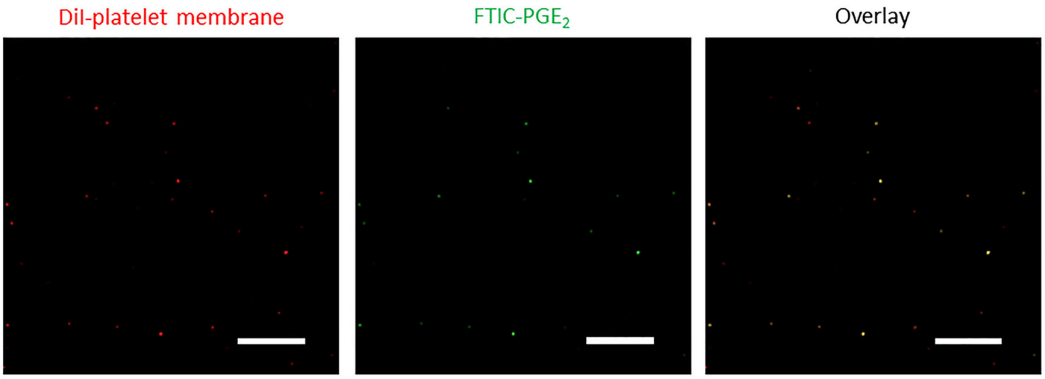

Figure S2. Confocal images of PGE_2-platelet membrane conjugate. The platelet membrane was labeled with DiI prior to the synthesis of PGE_2-platelet membrane conjugate. Subsequently, the DiI-labeled PGE_2-platelet membrane conjugate was incubated with FTIC-labeled PGE_2 antibody overnight before imaging. Scale bars, 10 μm.

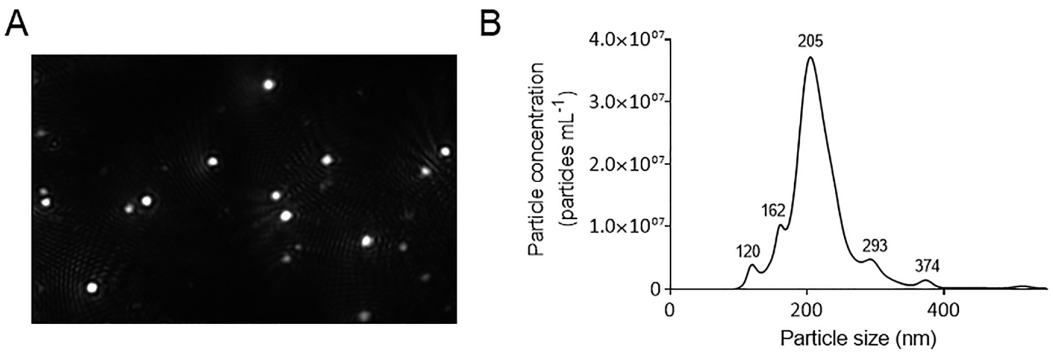

Figure S3. Nanoparticle tracking analysis (NTA) of CS-PGE$_2$-PINCs using NanoSight. (A) Representative particle tracking image of CS-PGE$_2$-PINCs; (B) Size distribution as reported by NTA showing that the average size of CS-PGE$_2$-PINC is about 205 nm, consistent with those determined by DLS and TEM analysis.

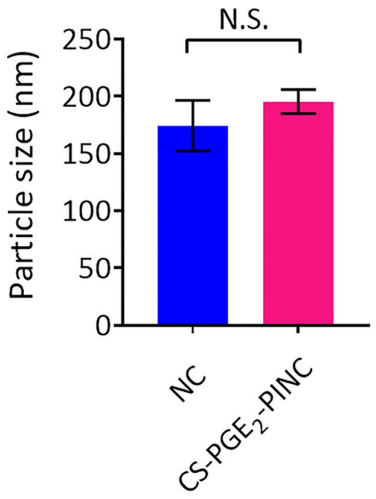

Figure S4. The average particle sizes of the as-prepared NCs and CS-PGE$_2$-PINCs in PBS (1×, pH 7.4). All data are mean ± s.d. (n = 3). Comparisons between any two groups were performed using two-tailed unpaired Student's t-test. N.S., no statistical significance.

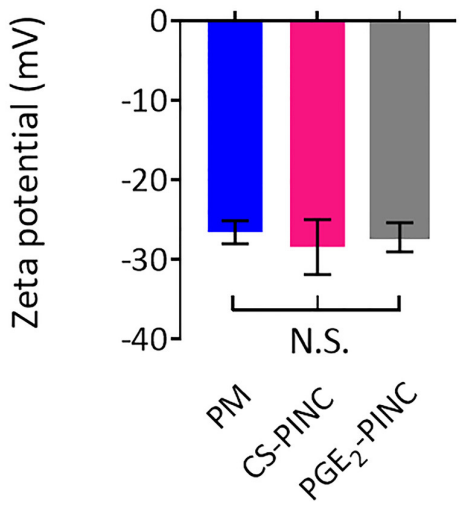

Figure S5. The zeta potentials of platelet membrane (PM), CS-PINCs, and PGE_2-PINCs in PBS (1×, pH 7.4). All data are mean ± s.d. (n = 3). Comparisons among more than two groups were performed using one-way ANOVA followed by *post hoc* Bonferroni test. N.S., no statistical significance.

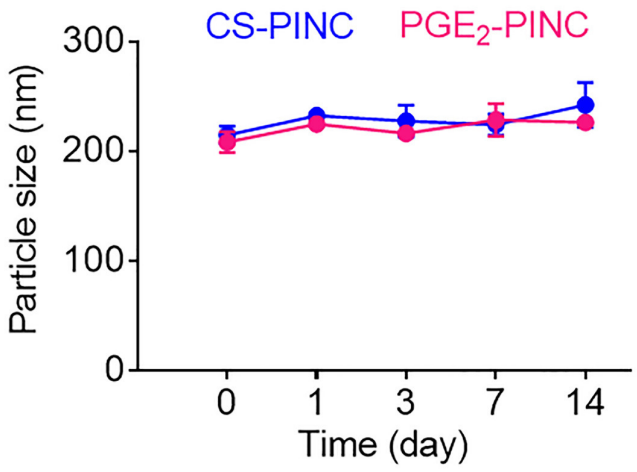

Figure S6. The average particle sizes of CS-PINC and PGE_2-PINC over 2 weeks in PBS (1×, pH 7.4). All data are mean ± s.d. (n = 3).

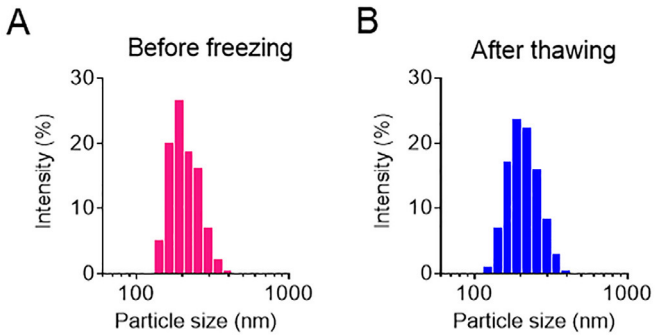

Figure S7. The particle size distribution of CS-PGE$_2$-PINC before freezing at -80 °C and after thawing at room temperature 3 months later.

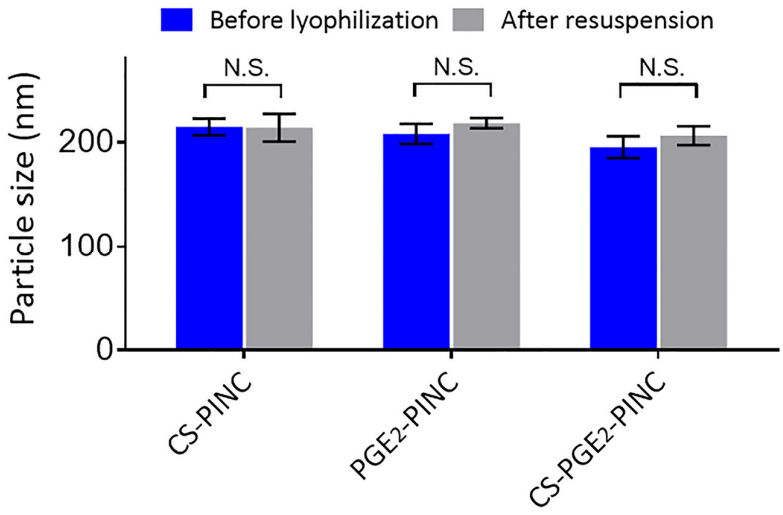

Figure S8. The particle sizes of CS-PINC, PGE_2-PINC, CS-PGE_2-PINC before lyophilization in 10 wt% sucrose and after resuspension in PBS (1×, pH 7.4). All data are mean ± s.d. (n = 3). Comparisons between any two groups were performed using two-tailed unpaired Student's t-test. N.S., no statistical significance.

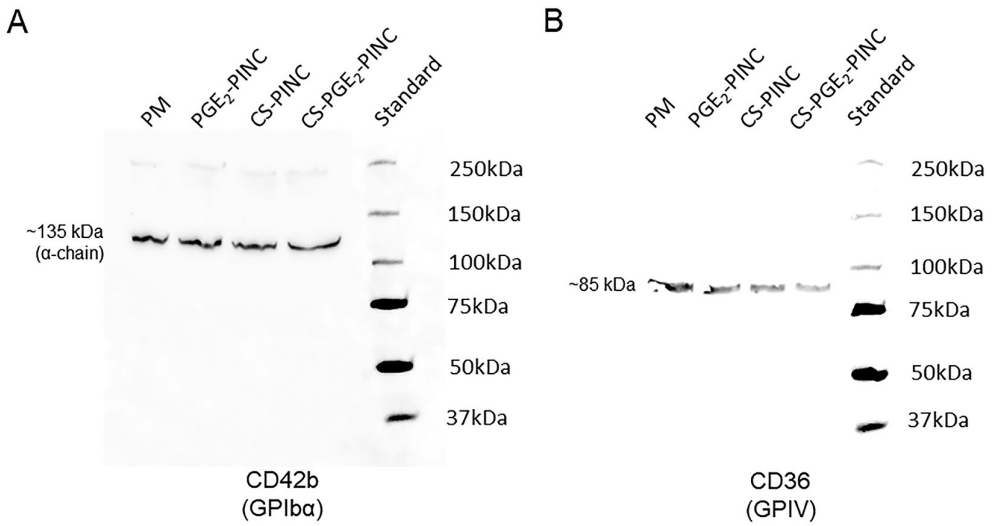

Figure S9. Western blot analysis of CD42b and CD36 in platelet membrane (PM), PGE_2-PINC, CS-PINC, and CS-PGE_2-PINC, respectively.

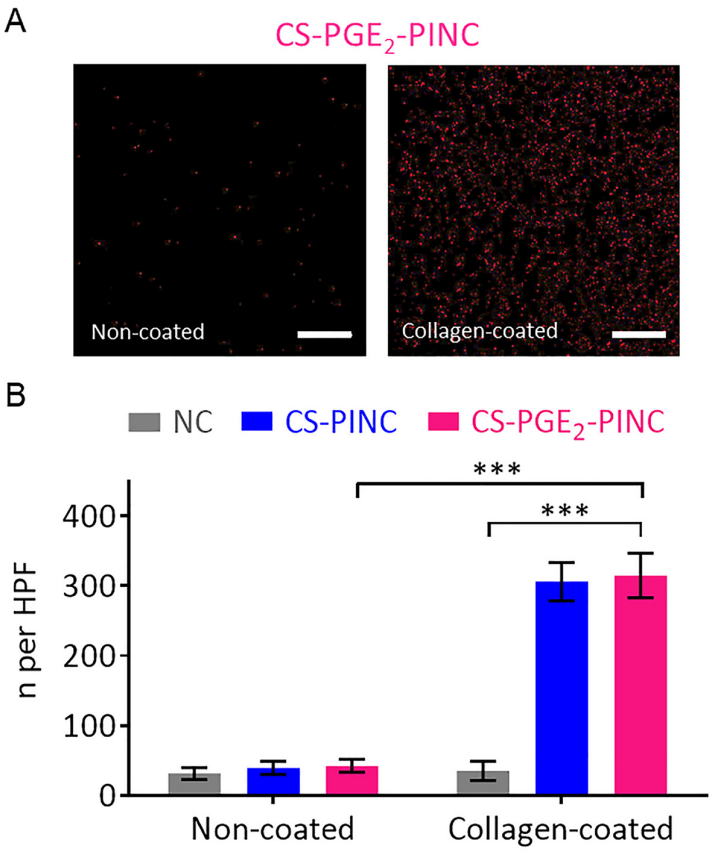

Figure S10. (A) Representative images showing the binding of CS-PGE2-PINCs to the collagen-coated 4-well culture chamber slide surface relative to the non-coated surface. (B) Quantification of the numbers of different nanoparticles binding to the collagen-coated and non-coated surfaces, respectively. All data are mean ± s.d. (n = 3). Comparisons between any two groups were performed using two-tailed unpaired Student's t-test. Comparisons among more than two groups were performed using one-way ANOVA followed by *post hoc* Bonferroni test. * indicates $p < 0.05$, ** indicates $p < 0.01$, *** indicates $p < 0.001$.

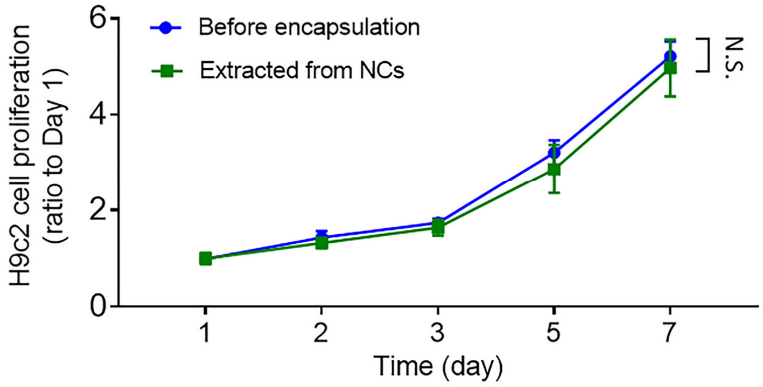

Figure S11. The effect of the native CSC secretome before encapsulation and that extracted from the CSC secretome-loaded PLGA nanoparticles (NCs) on the growth of H9c2 cardiomyoblasts over time. All data are mean ± s.d. (n = 3). Comparisons between any two groups were performed using two-tailed unpaired Student's t-test. N.S., no statistical significance.

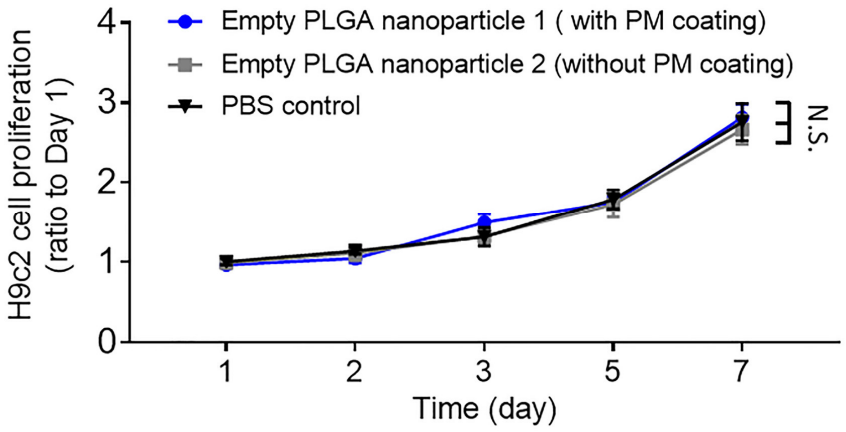

Figure S12. The proliferation of H9c2 cardiomyoblasts over time in the presence of the non-secretome-encapsulated empty PLGA nanoparticles with or without platelet membrane (PM) coating. All data are mean ± s.d. (n = 3). Comparisons among more than two groups were performed using one-way ANOVA followed by *post hoc* Bonferroni test. N.S., no statistical significance.

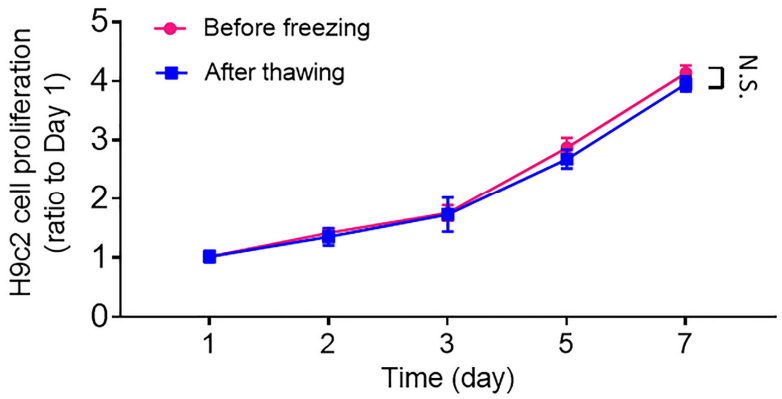

Figure S13. The effect of the CS-PGE$_2$-PINCs before freezing and those thawed after 3-month cryopreservation on the proliferation of H9c2 cardiomyoblasts over time. All data are mean ± s.d. (n = 3). Comparisons between any two groups were performed using two-tailed unpaired Student's t-test. N.S., no statistical significance.

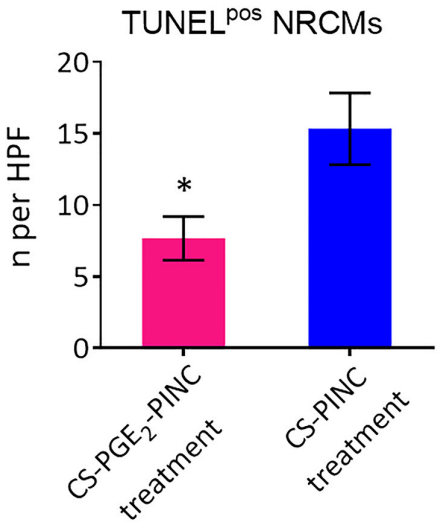

Figure S14. The apoptosis of CS-PGE_2-PINC-treated and CS-PINC-treated NRCMs after being exposed to serum-free IMDM medium supplemented with hydrogen peroxide (250 μM) for 3 h, as determined by TUNEL staining. All data are mean ± s.d. (n = 3). Comparisons between any two groups were performed using two-tailed unpaired Student's t-test. * indicates $p < 0.05$, ** indicates $p < 0.01$, *** indicates $p < 0.001$.

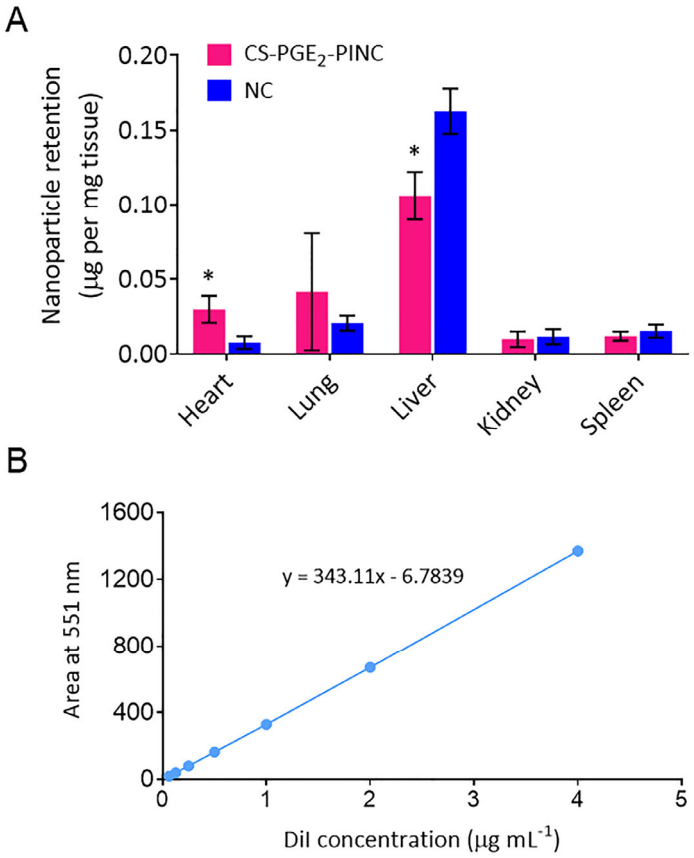

Figure S15. (A) HPLC analysis of nanoparticle retention in different organs normalized by tissue weight. (B) The standard curve constructed for determining the fluorescent dye concentration in different tissue samples.

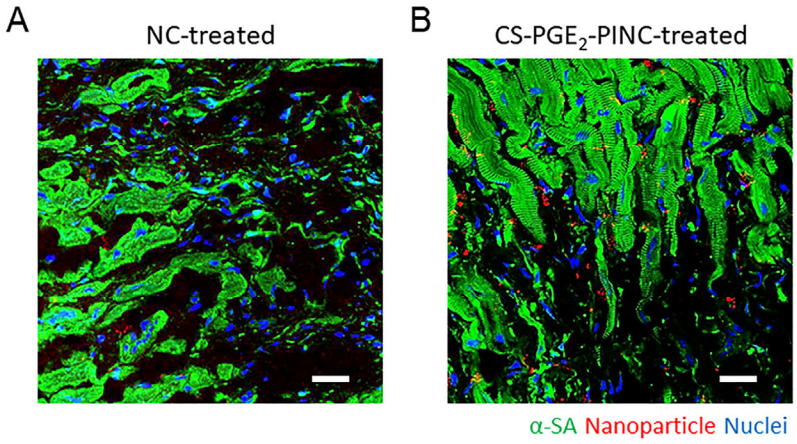

Figure S16. Representative immunofluorescence images showing nanoparticle (labeled with DiI) retention in the NC-recipient (A) and CS-PGE_2-PINC-recipient hearts (B), respectively, at 14 days post tail vein injection. Scale bar, 20 μm.

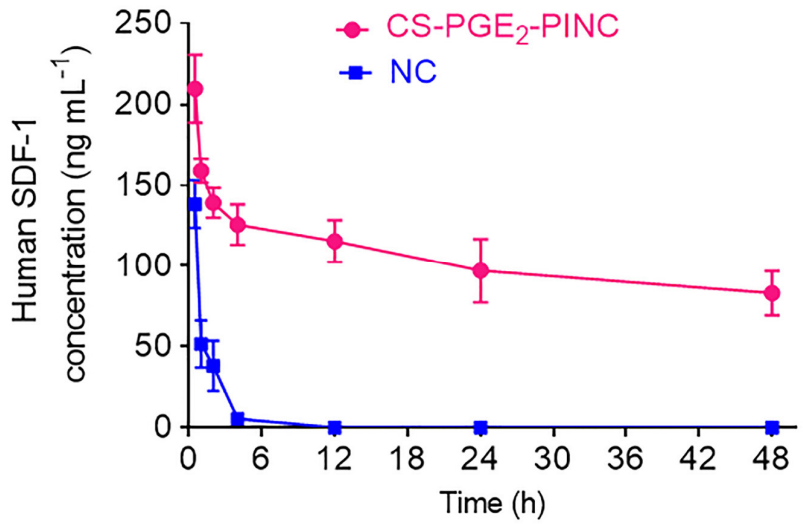

Figure S17. The plasma concentration of human SDF-1 released from CS-PGE_2-PINCs and NCs, respectively, after intravenous injection into mice with myocardial I/R injury over a span of 48 h (CS dose: 1.2 mg kg^{-1} mouse; PGE_2 dose: 0.053 mg kg^{-1} mouse). All data are mean ± s.d. (n = 3).

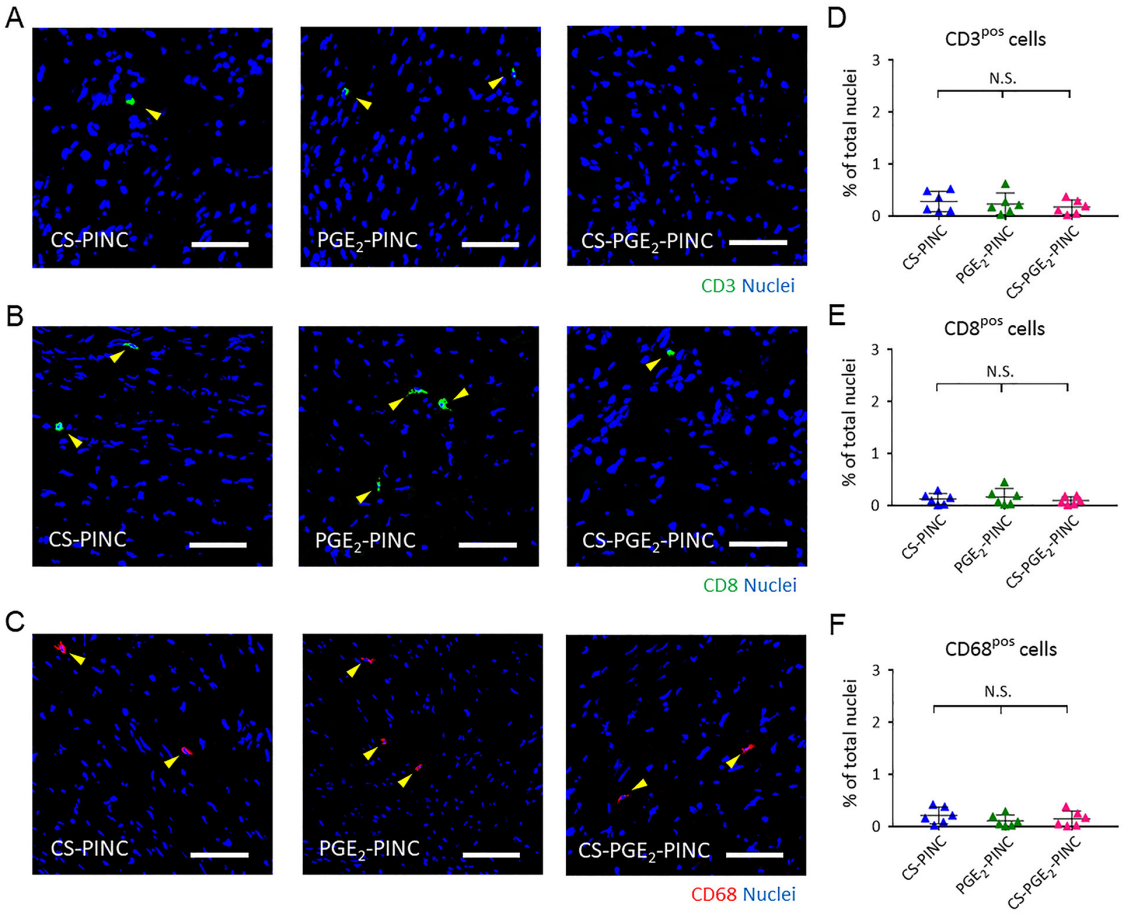

Figure S18. PINC injection does not stimulate local T-lymphocyte and macrophage immune response. The infiltration of T-lymphocytes with CD3 (green, A) and CD8 (green, B) expression was neglectable. Macrophages that labeled with CD68 (red, C) were also barely detected. Nuclei were counterstained with DAPI (blue). The numbers of CD3-positive (D), CD8-positive (E), and CD68-positive cells (F) were quantified. Scale bars, 50 μm. All data are mean ± s.d. (n = 6). Comparisons among more than two groups were performed using one-way ANOVA followed by *post hoc* Bonferroni test. N.S., no statistical significance.

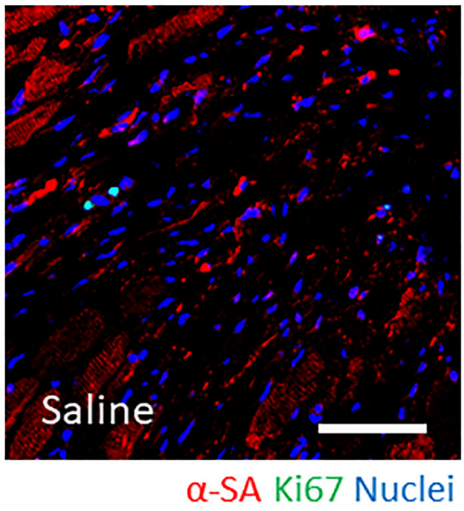

Figure S19. Representative images showing that cycling cardiomyocytes as indicated by α-SA and Ki67 double-positive staining were barely detected in the peri-infarct region of the hearts treated with saline at week 4. Scale bar, 50 μm.

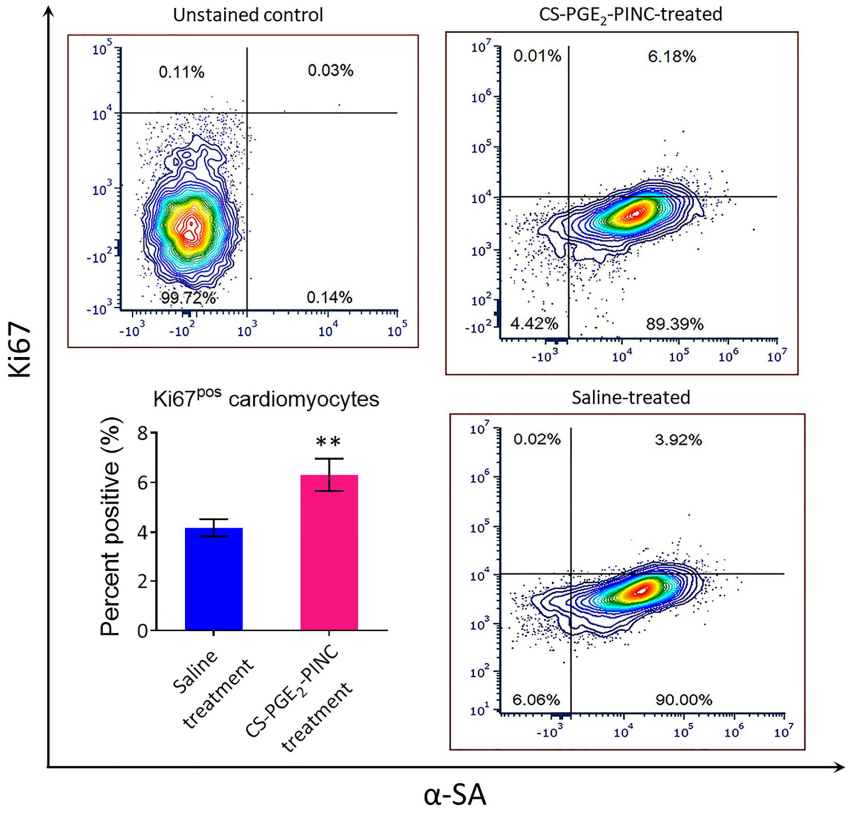

Figure S20. Flow cytometry analysis of Ki67$^+$ α-SA$^+$ cycling cardiomyocytes isolated from the mouse hearts treated with saline or CS-PGE$_2$-PINCs at 14 days post injection. The isolated cells were stained with Ki67 and α-SA for analysis. All data are mean ± s.d. (n = 3). Comparisons between any two groups were performed using two-tailed unpaired Student's t-test. * indicates $p < 0.05$, ** indicates $p < 0.01$, *** indicates $p < 0.001$.

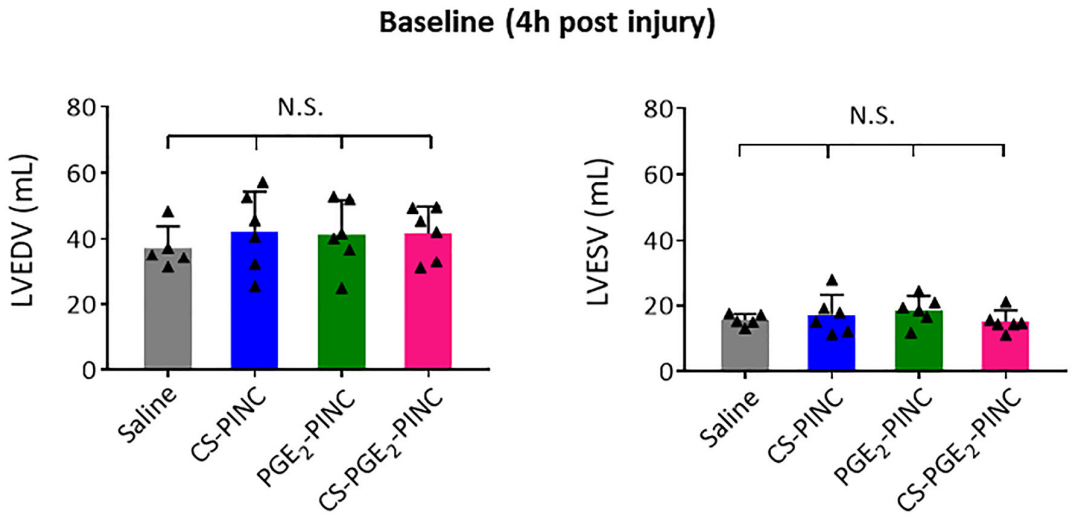

Figure S21. Left ventricular end-diastolic (left) and end-systolic (right) volumes (LVEDV and LVESV) measured by echocardiography at baseline (4h post I/R injury) in mice treated with saline, CS-PINCs, PGE_2-PINCs, and CS-PGE_2-PINCs, respectively. Comparisons among more than two groups were performed using one-way ANOVA followed by *post hoc* Bonferroni test. N.S., no statistical significance.